Check for updates

Biomechanical evaluation of different posterior fixation techniques for treating thoracolumbar burst fractures of osteoporosis old patients: a finite element analysis

Guodong Zhang[1,2†], Yukun Du[2†], Guangzong Jiang[1], Weiqing Kong[2], Jianyi Li[2], Zhongjiao Zhu[1]* and Yongming Xi[2]*

[1]Department of Spinal Surgery, Tengzhou Central People's Hospital, Tengzhou, China, [2]Department of Spinal Surgery, The Affiliated Hospital of Qingdao University, Qingdao, China

Objective: To investigate the biomechanical characteristics of different posterior fixation techniques in treatment of osteoporotic thoracolumbar burst fractures by finite element analysis.

Methods: The Dicom format images of T10-L5 segments were obtained from CT scanning of a volunteer, and transferred to the Geomagic Studio software, which was used to build digital models. L1 osteoporotic burst fracture and different posterior fixation techniques were simulated by SolidWorks software. The data of ROM, the maximum displacement of fixed segment, ROM of fractured L1 vertebrae, the stress on the screws and rods as well as on fractured L1 vertebrae under different movement conditions were collected and analysed by finite element analysis.

Results: Among the four groups, the largest ROM of fixed segment, the maximum displacement of fixed segment and ROM of fractured vertebrae occurred in CBT, and the corresponding data was 1.3°, 2.57 mm and 1.37°, respectively. While the smallest ROM of fixed segment, the maximum displacement of fixed segment and ROM of fractured vertebrae was found in LSPS, and the corresponding data was 0.92°, 2.46 mm and 0.89°, respectively. The largest stress of screws was 390.97 Mpa, appeared in CBT, and the largest stress of rods was 84.68 MPa, appeared in LSPS. The stress concentrated at the junction area between the root screws and rods. The maximum stress on fractured vertebrae was 93.25 MPa, appeared in CBT and the minimum stress was 56.68 MPa, appeared in CAPS. And the stress of fractured vertebrae concentrated in the middle and posterior column of the fixed segment, especially in the posterior edge of the superior endplate.

Conclusion: In this study, long-segment posterior fixation (LSPF) provided with the greatest stability of fixed segment after fixation, while cortical bone screw fixation (CBT) provided with the smallest stability. Cement-augmented pedicle screw-rod fixation (CAPS) and combined using cortical bone screw and pedicle screw fixation (CBT-PS) provided with the moderate stability. CBT-PS exhibited

superiority in resistance of rotational torsion for using multiple connecting rods. CAPS and CBT-PS maybe biomechanically superior options for the surgical treatment of burst TL fractures in osteoporotic patients.

Introduction

Spinal fracture, accounting for about 5% of systemic fractures, is often caused by car accidents, high falls and other injuries (Cahueque et al., 2016). The thoracolumbar (TL) region is mostly involved due to the major contributing factor of the biomechanical stress transitional area from the semirigid thoracic spine to the mobile lumbar spine. Because of the high-energy trauma, nearly 10%–20% TL fractures are burst fractures. The compression and fracture of the vertebral body has the increasing injury risk of spinal cord and nerve to affect the patients' life quality and labor ability (Hughes et al., 2021).

At present, conservative treatments including analgesia, bed rest and local immobilization are feasible for mild TL fracture patients without obvious neurological compromise and deformity. However, the delayed neurological deterioration of conservative treatments was reported up to 17% (Charles and Steib, 2015). Surgical interventions are most commonly recommended for burst TL fracture patients with neurological dysfunction and kyphosis. The main goal of surgical procedure is to provide patients with immediate spine stability, effectively neural decompression and kyphosis correction (Cook et al., 2021). With the aging of the population, the osteoporosis brings many challenges to treating the patient with burst TL fractures. The osteoporosis weakens the holding force of screws and obviously increases the risk of instrument failure. It was reported that the incidence of screw loosening was more than 60% of TL fracture patients with osteoporosis (Muratore et al., 2021).

There is still no consensus of the application guideline for different posterior fixation techniques in treatment of burst TL fractures with osteoporosis. Long-segment posterior fixation (LSPF) have advantages of better fixation strength and scattering stress, less possibility of spinal collapse and instrument failure. However, the extending fixation segment results in more surgical trauma and sacrifices more spinal motion segments, accelerating adjacent disc degeneration (Wang et al., 2019; Wu et al., 2019). The benefits of cement augmentation of pedicle screw fixation have been widely accepted. Compared with traditional screws, augmented by polymethylmethacrylate (PMMA) bone cement was able to improve the pullout resistance of screws in cancellous bone by 2–5 times. However, the complications including neural injury, pulmonary embolism and hypotension are still inevitable (Chevalier et al., 2021). Cortical bone screw is able to increase the screw holding force by adding more contact area between screw and cortical bone. Biomechanical experiments showed that CBT increase the axial stability of internal instrument nearly by 30% (Mai et al., 2016). Since firstly proposed by Santoni et al. (2009), the CBT technique is widely used in lumbar fusion with osteoporosis. However, it is rarely reported to be applied in burst TL fracture and the mechanical

performance is still unclear. The cross trajectory technique by combined using cortical bone screw and pedicle screw showed the advantages of increasing fixation strength of pedicle screws, reducing the fixation segments as well as retaining the range of spine motion (Matsukawa et al., 2015), which may provide another reliable measurement to burst TL fracture.

To evaluate the biomechanical characteristics of different posterior fixation techniques, we simulated the finite element model of osteoporotic burst L1 fracture and conduct the finite element analysis of four different fixation techniques including cement-augmented pedicle screw fixation (CAPS), long-segmented pedicle screw fixation (LSPS), cortical bone screw fixation (CBT) and combined using cortical bone screw and pedicle screw fixation (CBT-PS). Under different movement conditions, data of ROM, maximum displacement of fixed segment, ROM of fractured L1 vertebrae, stress on instrument and fractured vertebrae were collected to compare the effectiveness of different posterior fixation techniques in treatment of burst TL fracture patients with osteoporosis, which provided theoretical basis for clinical application. The report is listed as follows.

Materials and methods

The establishment of intact models of T10-L5

One healthy 29-year-old male volunteer was enrolled in this study. The volunteer assigned the informed consent form before the study. This study was approved by the ethics committee of the affiliated hospital of Qingdao University (Ethics No. QYFYKYLL911411930).

The 64-slice spiral computed tomography scanner (Siemens, Germany) was used to scan this volunteer from the T10 to L5 vertebrae levels. The finite element (FE) model of the thoracolumbar from T10 to L5 was established as follows: 1) the CT images were scanned and the Dicom data was imported into Mimics Software 21.0 (Materialise, Leuven, Belgium) and the vertebral boundaries as regions of interest were identified with multiple images to form a 3-node triangular surface model. 2) The surface model was imported from SolidWorks (SOLIDWORKS Corporation, Boston, Massachusetts, United States) to further reconstruct a 3-dimensional solid model of the T10-L5 segment. 3) The solid model of the thoracolumbar spine was imported into Geomagic Wrap Software (Geomagic, Cary, North Carolina, United States) to optimize model shape, fit surface and build surface model. The nucleus pulposus and annular fibers were built separately. Intervertebral disc models of osteoporosis was

TABLE 1 Materials Property of the finite element model.

| Element	Young's modulus (MPa)	Poisson's ratio	Cross-sectional area (mm^2)
Cortical bone (osteoporosis)	8,040	0.3	—
Cancellous bone (osteoporosis)	34	0.2	—
Endplate	1,000	0.3	—
Cartilage	50	0.3	—
Annulus fibrosus	5	0.45	—
Nucleus pulposus	9	0.4	—
Screws and rods	110,000	0.28	—
Bone cement	3,000	0.4	—
Anterior ligaments	20	0.3	63.7
Posterior ligaments	20	0.3	20
Flavum ligaments	19.5	0.3	40
Intertransverse ligaments	12	0.3	40
Interspinal ligaments	15	0.3	30
Supraspinal ligaments	59	0.3	3.6
Capsular ligaments	75	0.3	60
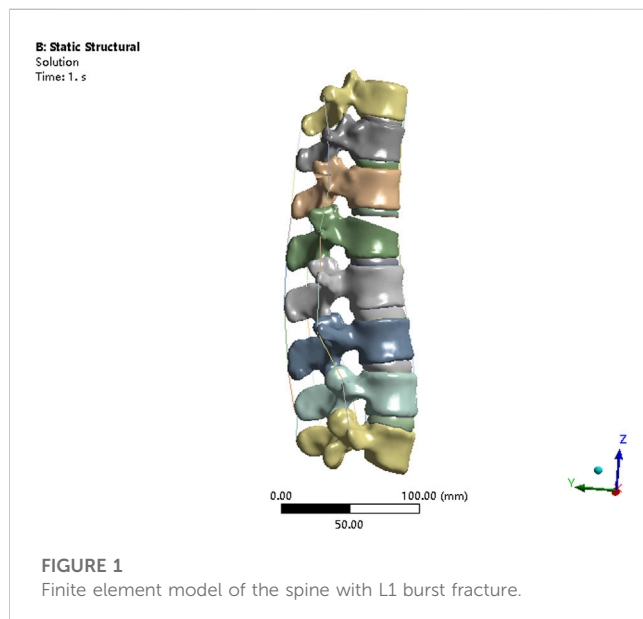
FIGURE 1
Finite element model of the spine with L1 burst fracture.

simulated by the description of Sungwook Kang's study (Kang et al., 2022). The volume ratio of the annulus fibrosus to the nucleus pulposus was set to 6:4. The thickness of vertebral cortical bone and endplate were set to 0.7 mm. The contact property of facet joint surface was set to tangential action without friction, and the initial gap of facet joint was set to 0.5 mm. The models of paraspinal ligaments (the anterior longitudinal ligament, the supraspinous ligament and the intertransverse ligament) were established by using Workbench (Ansys, Pittsburgh, Pennsylvania, United States). The parameters of material properties were used in this study shown on the Table 1. 4) The final FE models were imported to Abaqus FE analysis software (Abaqus, Simulia Corp., Providence, Rhode Island, United States) for analysis.

The establishment of thoracolumbar burst fracture models in osteoporotic condition

The V-shaped osteotomy of L1 vertebral body was performed by SolidWorks to simulate burst L1 fracture. The upper two-thirds of the anterior sponge bone of L1 vertebra was removed to weaken the vertebral strength, as described by Basaran et al. (2019). The anterior longitudinal ligament and posterior longitudinal ligament were discontinuous to fully simulate burst L1 vertebrae fracture (Figure 1). The material properties for the osteoporotic bony structures were reduced, compared with normal bony structures, by 66% of the elastic modulus for cancellous bone and by 33% for cortical bone, bony endplate, and posterior elements, as described by Guo et al. (2020).

The finite element models of different internal fixations

The models of screws (55 mm × 45 mm/55 mm × 40 mm) and rods (diameter of 5 mm) were respectively constructed by SolidWorks software. Pedicle screws of thoracolumbar vertebrae were inserted by using the herringbone crest vertex technique. Based on the study brought by Santoni et al. (2009), the cortical bone screws were inserted.

Four finite element models of different posterior fixation techniques were simulated in this study. CAPS: Pedicle screws (55 mm × 45 mm) were inserted bilaterally in pedicles of T12,
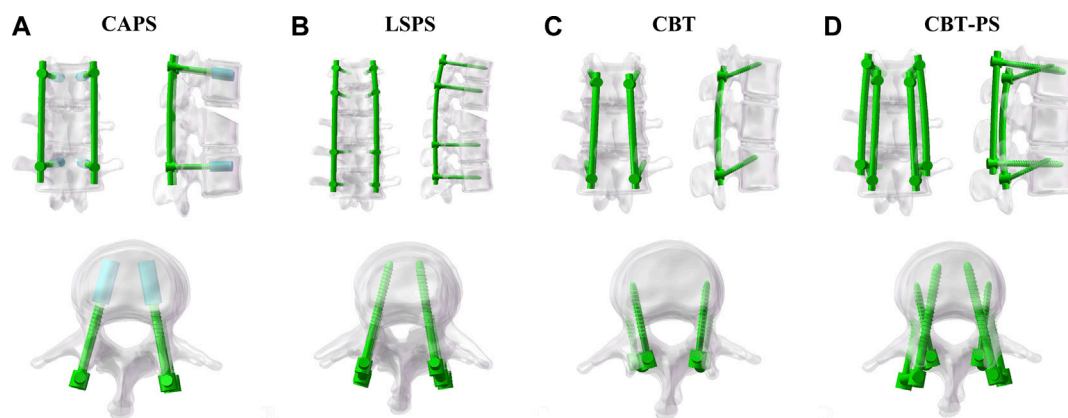
FIGURE 2
The four different posterior fixation models including CAPS, LSPS, CBT and CBT-PS.

L2 vertebral arch. A cylindrical cement was built along each pedicle screw to the distal end and the volume of cement was set as 1 mL, as described by Wenhai Wang (Wang et al., 2014); LSPS: Pedicle screws (55 mm × 45 mm) were inserted bilaterally in pedicles of T11, T12, L2 and L3 vertebral arch; CBT:Cortical bone screws (55 mm × 40 mm) were inserted bilaterally in T12, L2 vertebra cortex; CBT-PS: Cortical bone screws (55 mm × 40 mm) and pedicle screws (55 mm × 45 mm) were inserted simultaneously in one vertebra cortex and vertebral arch in T12, L2 (Figure 2).

Boundary conditions and loads

The lower edge of L5 vertebral body was fixed to limit the movement of L5 lower endplate in different directions. 500 N load was applied vertically above the T10 vertebral body, and 7.5 Nm was applied on the upper surface of the T10 vertebral body to simulate the movement including flexion, extension, bending and rotation. Range of motion (ROM), maximum displacement of fixed segment, ROM of fractured L1 vertebrae, stress distribution on constructs and fractured L1 vertebrae were analyzed under six movement conditions of flexion, extension, left bending, right bending, left rotation and right rotation, respectively.

Results

Validation of the intact T10-L5 finite element model

In order to evaluate the validity of T10-L5 intact model, 7.5 Nm torque was applied to the model to simulate the force under physiological load. Under the conditions of flexion, extension, left bending, right bending, left rotation and right rotation, the ROM of T10-L5 spinal intact model was 5.31˚, 5.63˚, 4.81˚, 4.91˚, 3.14˚, 3.51˚, respectively, which was comparable with the experimental data reported by Pflugmacher et al. (2004) and Basaran et al. (2019) to validate the rationality of the models (Table 2).

TABLE 2 Comparison between the normal spine model and models from previous studies.

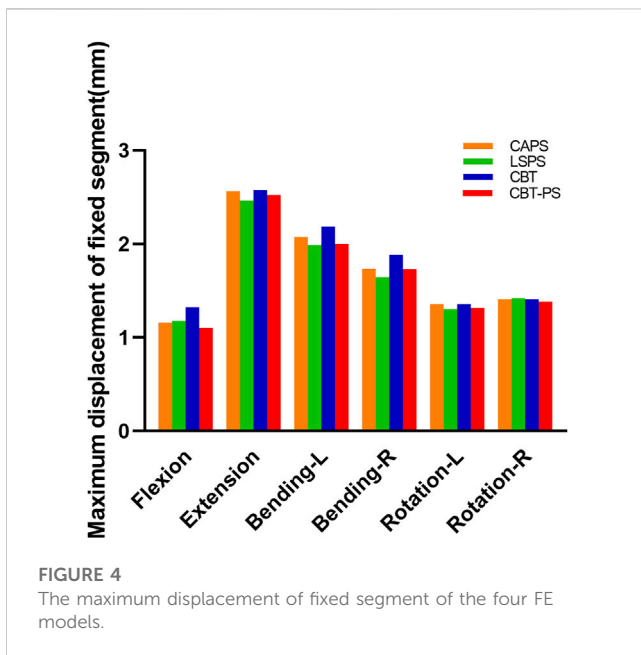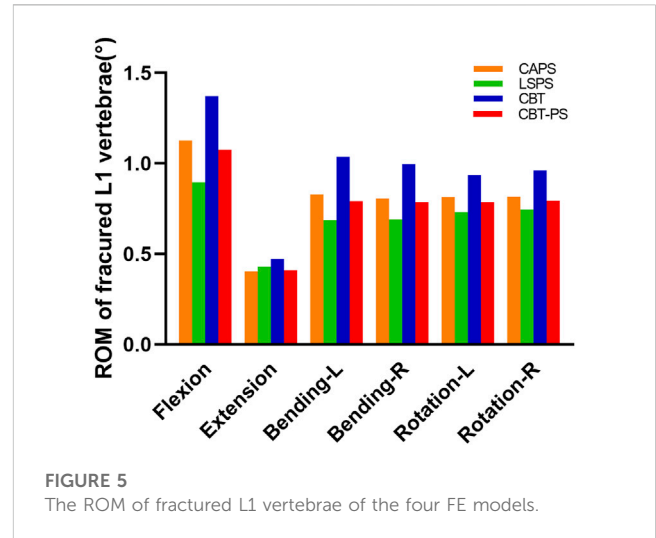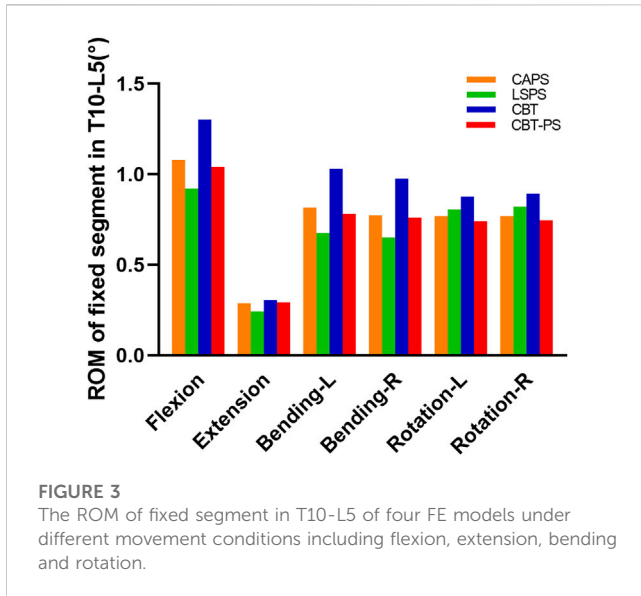|	ROM(˚)		
	Present Study	Pflugmacher et al.	Basaran et al.
Flexion	5.31	5.3 ± 1.0	4.5 ± 0.9
Extention	5.63	5.7 ± 1.0	4.5 ± 0.9
Left bending	4.81	4.3 ± 0.6	4.2 ± 0.8
Right bending	4.91	4.3 ± 0.6	4.2 ± 0.8
Left rotation	2.14	2.1 ± 0.5	2.3 ± 0.6
Right rotation	2.51	2.1 ± 0.5	2.3 ± 0.6

Date from present study is comparable with the results from previous research.

ROM of fixed segment in four FE fixation models

A significant decrease in ROM of fixed segment was found after fixation. The largest ROM in each group appeared under the movement of flexion and the smallest ROM was under extension.

The largest ROM of fixed segment was 1.3˚, appeared in CBT. While the smallest ROM was 0.92˚, appeared in LSPS. Among the four groups, CBT had the largest ROM in six directions and LSPS had the smallest ROM in directions of flexion, extension, left bending and right bending. Compared with CBT, CAPS had a decrease of 17.08% in flexion, 5.97% in extension, 20.78% in left bending, 20.58% in right bending, 12.28% in left rotation and 14.14% in right rotation. Compared with CBT, CBT-PS had a decrease of 20.11% in flexion, 4.19% in extension, 24.18% in left bending, 21.91% in right bending, 15.28% in left rotation and 16.43% in right rotation (Figure 3).

In addition, the decreased percentage of ROM after fixation in all groups was compared to assess the ability of stability restoration. CBT had the lowest decreased percentage in six directions (decreased by 67.01% in flexion, 92.61% in extension, 71.81% in left bending, 72.35% in right bending, 70.78% in left rotation, 66.74% in right rotation). The most obvious decreased percentage of ROM was found in LSPS in most

FIGURE 3
The ROM of fixed segment in T10-L5 of four FE models under different movement conditions including flexion, extension, bending and rotation.

FIGURE 4
The maximum displacement of fixed segment of the four FE models.

directions except for axial rotation (decreased by 87.30% in flexion, 97.02% in extension, 90.45% in left bending, 90.97% in right bending).

The larger ROM and smaller decreased percentage after fixation in CBT means more abnormal movement compared with other techniques. So the stability of fixed segment in LSPS was best, while the worst stability occurred in CBT. The stability of CAPS and CBT-PS was between LSPS and CBT.

The maximum displacement of fixed segments in four FE fixation models

The maximum displacement of fixed segment was defined as the max perpendicular distance between the posterior of upper and

FIGURE 5
The ROM of fractured L1 vertebrae of the four FE models.

bottom vertebrae. In the research, we found that the maximum displacement of fixed segment decreased after fixation in all groups. The largest maximum displacement of fixed segment was 2.57 mm, appeared in CBT. The smallest maximum displacement was 2.46 mm, appeared in LSPS.

LSPS has the smallest and CBT has the largest maximum displacement of fixed segment in most directions except for right rotation. Compared with CBT, CAPS had a decreased by 12.61% in flexion, 0.46% in extension, 4.9% in left bending, 7.9% in right bending, 0.9% in left rotation. Compared with CBT, CBT-PS had a decreased by 16.65% in flexion, 2.01% in extension, 8.27% in left bending, 8.28% in right bending, 3.05% in left rotation and 1.57% in right rotation. Interestingly, the largest maximum of fixed segment under right rotation occurred in LSPS (Figure 4).

The larger maximum displacement means the worse stability after fixation. In accordance with the results of ROM described above, the best stability occurred in LSPS and the worst was in CBT. The fixed segment in CAPS and CBT-PS had similar stability, which located between the stability of LSPS and CBT. However, it should be noted the largest maximum displacement in LSPS under the movement of right rotation may imply the disability to withstand excessive right rotation.

ROM of fractured L1 vertebrae

ROM of fractured L1 vertebrae was recorded by measuring the Cobb angle variation of L1 vertebrae. The maximum ROM of fractured L1 vertebrae appeared under the movement of flexion, while the minimum ROM appeared under the movement of extension.

The largest ROM of fractured L1 vertebra was 1.37°, appeared in CBT. And the smallest ROM of fractured L1 vertebrae was 0.89°, appeared in LSPS. CBT had the largest ROM of fractured L1 vertebrae in six directions and LSPS had the lowest ROM in most directions except for extension. Compared with CBT, CAPS had a decrease by 17.2% in flexion, 14.78% in extension, 19.99% in left bending, 18.99% in right bending, 13.24% in left rotation and 15.02% in right rotation. Compared with CBT, CBT-PS had a decrease by 21.41% in flexion, 13.41% in extension, 23.66% in

TABLE 3 Maximum von Mises stress in the pedicle screws and rods.

		CAPS	LSPS	CBT	CBT-PS
Screws	Stress (MPa)	191.45	82.829	390.97	214.66
	Motion	Flexion	Left bending	Flexion	Flexion
	Level	T12	L3	T12	T12
Rods	Stress (MPa)	62.156	84.68	73.026	62.201
	Motion	Left bending	Right bending	Right bending	Left bending

left bending, 20.89% in right bending, 16.20% in left rotation and 17.38% in right rotation (Figure 5).

The von Mises stress on the screws and rods

The maximum von Mises stress of screws in CAPS, LSPS, CBT, CBT-PS was 191.45, 82.82, 390.97, and 214.66 MPa, respectively. The largest stress of screws was 390.97 MPa, appeared in CBT under the movement of flexion. Compared with CBT, the maximum von Mises stress of screws in LSPS, CAPS, CBT-PS decreased by 78.81%, 51.03% and 45.09%, respectively (Table 3).

For the rods, the maximum von Mises stress in CAPS, LSPS, CBT, CBT-PS was 62.15, 84.68, 73.02, and 62.20 MPa, respectively. The largest von Mises stress was 84.68 MPa, appeared in LSPS under the movement of right bending. Compared with LSPS, the maximum von Mises stress in CAPS, CBT-PS and CBT decreased by 26.59%, 26.54% and 13.76%, respectively (Figure 6).

The nephogram of the maximum von Mises stress in all models concentrated at the junction area between root of screws and the connecting rods.

The von Mises stress on fractured L1 vertebrae body

The maximum von Mises stress of fractured L1 vertebral appeared under the movement of flexion and the minimum stress appeared under extension. The maximum von Mises stress in CAPS, LSPS, CBT, CBT-PS was 56.68, 82.55, 93.25, and 71.75 MPa, respectively. The largest maximum stress was 93.25 MPa, appeared in CBT under the movement of flexion. Compared with CBT, the maximum stress on fractured L1 vertebrae in CAPS, CBT-PS and LSPS decreased by 39.21%, 23.05% and 11.47%, respectively.

The nephogram of the maximum von Mises stress of fractured L1 vertebrae was concentrated in the middle and posterior column of the fixed segment, especially in the posterior edge of the superior endplate (Figure 7).
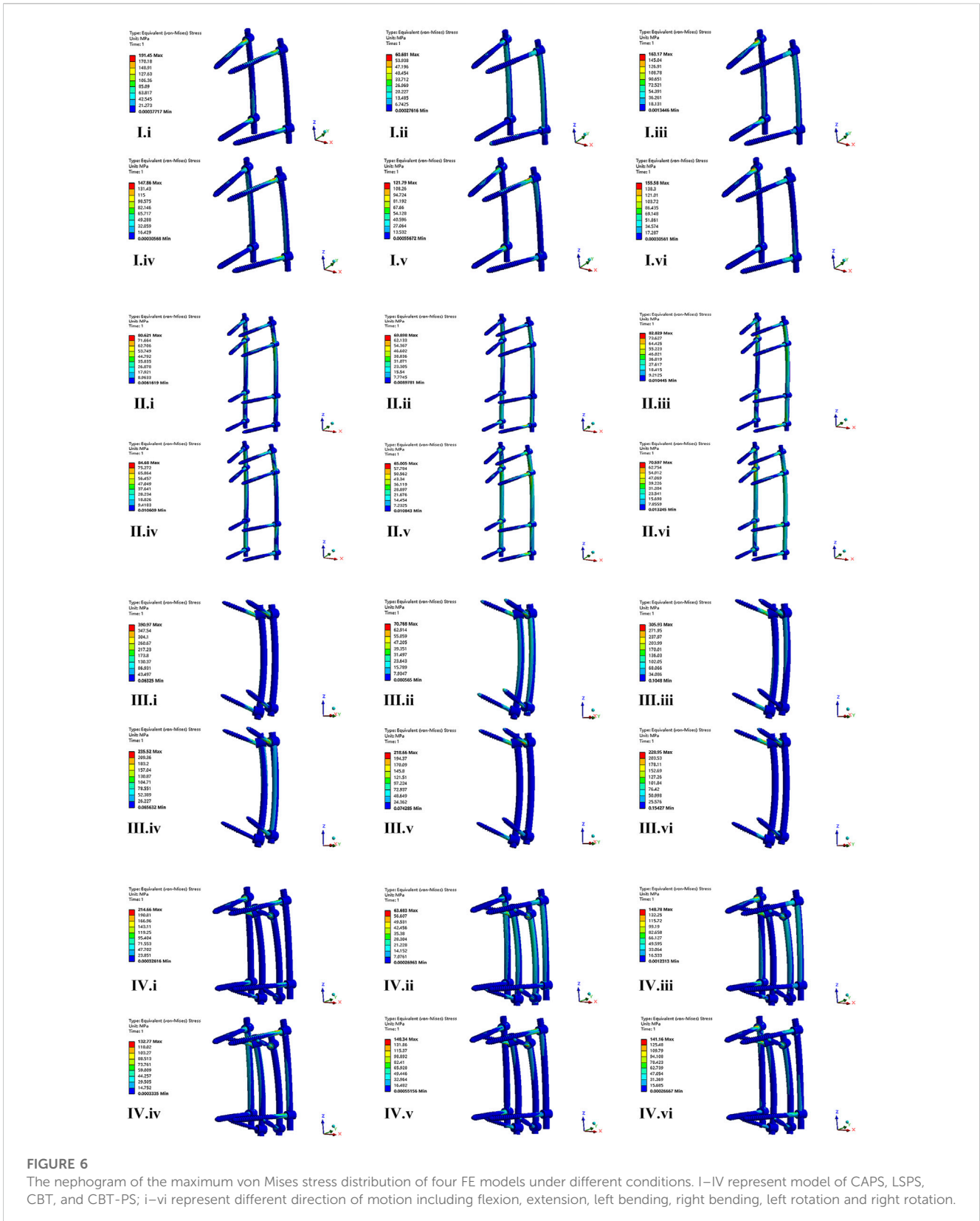
Discussion

As to the treatment of TL burst fractures, surgical intervention was indicated to provide patients with immediate stability, correction of kyphosis and effectively decompression of spinal cord and nerve. Posterior pedicle screw fixation system was regarded as an efficient method for the treatment of TL burst fractures. However, it should be

cautious when the osteoporotic patients may suffer from instrument failure due to the negative influence of decreasing hold screw force (Liao, 2020). Maintaining adequate fixation strength is necessary to accelerate fracture healing and avoid pseudarthrosis. However, there is still no consensus of the application guideline for different posterior fixation techniques in treatment of burst TL fractures.

In present study, the FE analysis was conducted to compare biomechanical characteristics of different posterior fixation techniques to provide theoretical evidence for clinical application in treatment of burst TL fractures with osteoporosis. As described by Wang et al. (2014), we constructed cement-augmented fixation (CAPS) models. Briefly, the suitable PMMA cement (1 mL) was constructed along the pedicle screw to the distal end, and cement located in anterior and middle column of vertebrae mostly to avoid cement leakage. In his survey, it is observed that insertion of 1.0 cm^3 cement causes pullout forces to increase by 50.7% and 60.8% for spherical and cylindrical cement volumes, respectively. When 2.5 cm^3 of cement is inserted, the pullout forces are increased by approximately 116% and 120% for spherical and cylindrical cement zones, respectively (Wang et al., 2014). However, from our practical clinical experience, a bigger volume (2.5 mL) of cement is too larger to causing difficulty in cement insertion and inducing some complications, such as cement leakage and neurological deterioration. Based on the proof discussed above, we simulated cement augmentation models by inserting 1.0 cm^3 cylindrical cement during the FE experiment. And we found that the fixation strength of pedicle screws increased after cement augmentation, which lead to a moderate stability of fixed segment. The balloon kyphoplasty (KP) with PMMA cement injection in fractured vertebrae is another method of cement augmentation. Shady Elmasry conducted an experiment to evaluate biomechanical perfomance of stand-alone KP, stand-alone percutaneous pedicle screws fixation (PPSF) and KP-augmented PPSF. However, the biomechanical superiority of KP-augmented PPSF over the stand-alone PPSF was not confirmed in that study (Elmasry et al., 2018).

Although CBT have been seen as one of the remedial surgical methods in osteoporotic patients, the mechanical result of CBT in our survey was not satisfactory. ROM and maximum displacement of fixed segment was largest under every movement condition, indicating the worst stability of fixed segment after fixation, which maybe caused by the insufficient support of anterior column. Matsukawa et al. found the stability after CBT fixation was worse under rotation and lateral bending movement condition (Sakaura et al., 2016). Although Sellin et al. (2018) demonstrated preferable results of the use of CBT to treat unstable traumatic thoracolumbar fractures, but this result based on fewer cases was more susceptible.

In addition, the result of our study showed the CBT-PS technique can supply with moderate stability of fixed segment

FIGURE 6
The nephogram of the maximum von Mises stress distribution of four FE models under different conditions. I–IV represent model of CAPS, LSPS, CBT, and CBT-PS; i–vi represent different direction of motion including flexion, extension, left bending, right bending, left rotation and right rotation.

and exhibit superiority in resistance of rotational torsion. The CBT-PS technique is a reliable and useful technique to reinforce the fixation strength for creating multiple points of fixation within a vertebrae. Combined using pedicle screw and cortical bone screw

simultaneously can make up the shortcomings of insufficient fixation strength of CBT (Ueno et al., 2013). Michal Szczodry in his survey pointed out that the increased cortical purchase (ICP) insertion technique results in same biomechanical performance and
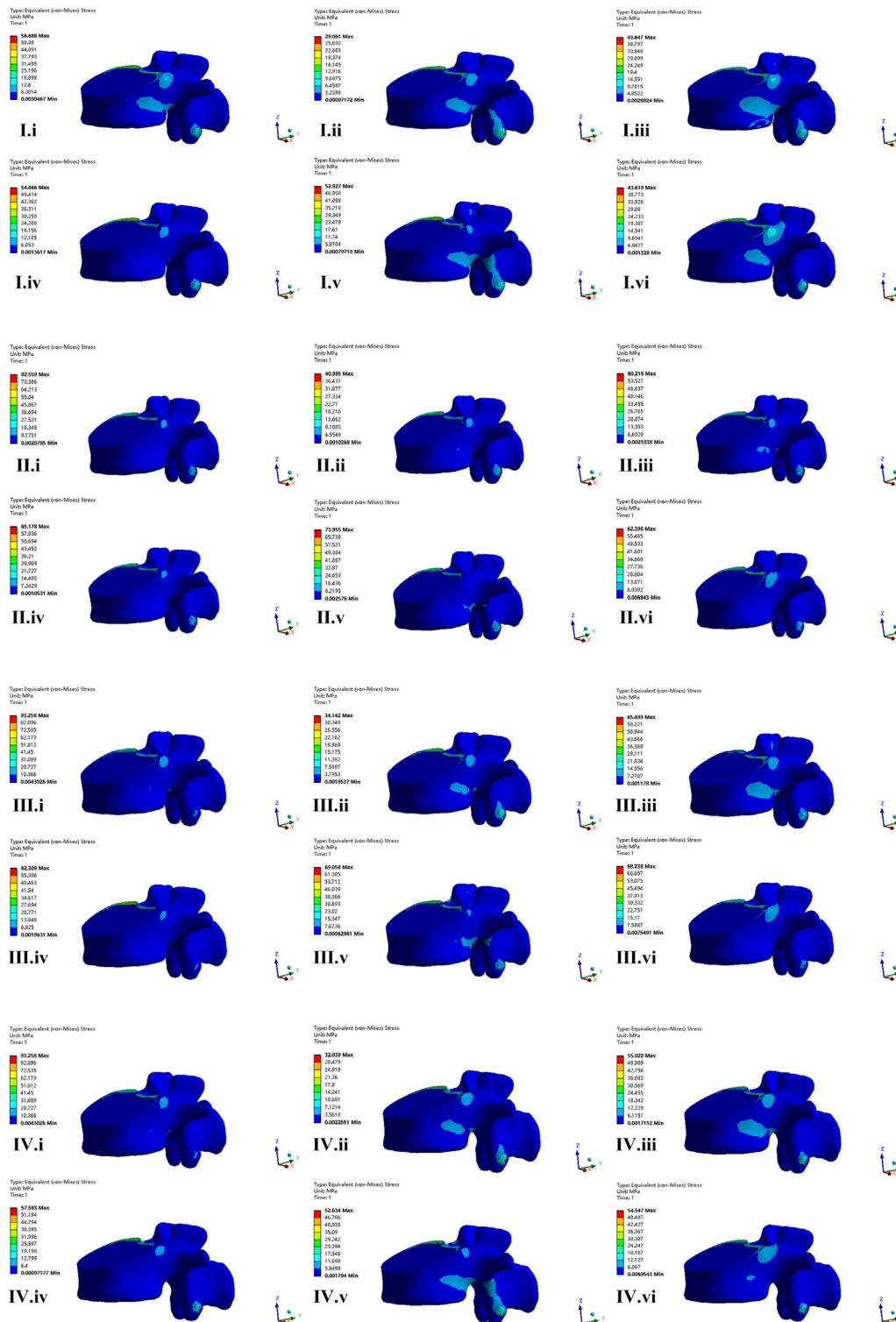
FIGURE 7
The nephogram of the von Mises stress distribution of fractured vertebrae body of four FE models. I–IV represent model of CAPS, LSPS, CBT, and CBT-PS; i–vi represent different direction of motion including flexion, extension, left bending, right bending, left rotation and right rotation.

same accuracy as the straightforward technique by using guidance (Szczodry et al., 2018). However, the difficulty of inserting CBT and pedicle screw is a common problem confronted in practical use. At first, the pedicle size need to be large enough to accommodate two

screws in one pedicle. In our study, the selected pedicle screws were 5.5 mm in diameter and 50 mm in length; the CBT screws were 5.5 mm in diameter and 40 mm in length, which was in accordance with Keitaro Matsukawa's survey (Matsukawa et al., 2015). And

then, choosing the ideal screw path for the optimal fixation plays an important role in the cross-trajectory technique. With the development of technology, difficulties in inserting screw safely and pricisely can be overcomed with the use of appropriate technologies. In a cadaver study, individualized surgical guide templates for double-trajectory screw placement were designed and the result was satisfactory (Zhao et al., 2021).

Previous studies have shown that the pedicle screw fixation system converts 50% axial pressure of the vertebral body into the pressure on the screw and connecting rod in lumbar fusion (Spiegl et al., 2022). In burst TL fractures, the more pressure on the screw caused by the loss of anterior and middle column support increased the risk of instrument failure. In this study, the largest stress on screws occurred in CBT, and the smallest stress was in LSPS. The worse stability in CBT means more abnormal movement, which exert more stress on instruments. Adding additional screws and augmentation with cement can scatter the screw stress effectively. For the rods, the largest stress occurred in LSPS. Extending fixed segment lead to the increase of stiffness and local stress concentration. What's more, we found that the maximum stress of the screw concentrate at junction area between the root of the screw and the connecting rod, which is consistent with previous study (Wu et al., 2019). Although the peak stress of screw and connecting rod do not exceed the 529 MPa endurance limit of titanium alloy (Wycisk et al., 2014), the spine is a relatively active unit and local fretting exert the continuous stress of internal instrument increasing the risk of fatigue fracture.

The axial compression pressure was delivered downward to the fractured vertebral body. The excessive stress on the fractured vertebral body has the negative effect on fracture healing. In this research, the stress on fractured vertebrae under flexion movement was bigger than other movement condition. The largest stress on fractured vertebrae occurred was found in CBT, caused by the poor ability to restore stability of fixed segment. CAPS has the smallest stress on fractured vertebrae, which is resort to the fact more points of fixation on vertebral make the stress more dispersed rather than concentrated. In addition, bone cement has inherent advantages of bone induction for bone growth, which is beneficial to recovery from burst fracture (Cai et al., 2023).

FE analysis is a reliable and helpful method to predict mechanical strength and dynamic characteristics of simulated constructs. However, there are many aspects of influencing factors in the process of FE analysis. Osteoporosis is clinically related to an age-related degeneration process, cell density, nutrition level, proteoglycans (PGs), water contents, as well as volume change in the disc decreased over the progression of degeneration across decades, as discussed by Mallory Volz (Volz et al., 2021). In our study, we built osteoporotic models of intervertebral disc, and the model was validated with others' literature. In addition, instrument properties such as metal material, craft of surface coating may have an effect on the result of FE analysis. Patrick A. Massey compared the biomechanical performance of nitinol memory metal rods and titanium rods. He found that nitinol trended toward superior fatigue resistance, but there was no significant difference in nitinol versus titanium construct fatigue resistance (Massey et al., 2021). In an experiment of SWEETU PATEL, the nanotubes surface were inserted at Ti6Al4V rod, and the stability between the bone-implant interface was promoted (Patel et al., 2015).

There are some limitations in our study. First, the finite element model is constructed by obtaining the CT data of a single patient and hardly represent the biomechanics of different ages and genders. Second, the current finite element model does not include the spinal muscle system, which plays an important role in maintaining the stability of the spine. At last, increasing the diameter and length of the screw can potentially produce larger pullout forces but may also increase the risk of fracturing the surrounding fragile bone (Solitro et al., 2019). The mechanical performance was not included in this study. The further biomechanical experiments in cadaver studies and clinical cohort studies would be needed to be performed to prove the results of this study.

Conclusion

In this study, long-segment posterior fixation (LSPF) provided with the greatest stability of fixed segment after fixation, while cortical bone screw fixation (CBT) provided with the smallest stability. Cement-augmented pedicle screw-rod fixation (CAPS) and combined using cortical bone screw and pedicle screw fixation (CBT-PS) provided with the moderate stability. CBT-PS exhibited superiority in resistance of rotational torsion for using multiple connecting rods. CAPS and CBT-PS maybe biomechanically superior options for the surgical treatment of burst TL fractures in osteoporotic patients.

Data availability statement

The raw data supporting the conclusion of this article will be made available by the authors, without undue reservation.

Author contributions

GZ: Writing–original draft, Writing–review and editing. YD: Writing–original draft, Writing–review and editing. GJ: Software, Writing–review and editing. WK: Data curation, Supervision, Writing–review and editing. JL: Software, Validation, Writing–original draft. ZZ: Project administration, Supervision, Writing–review and editing. YX: Methodology, Software, Supervision, Writing–review and editing.

Funding

Conflict of interest

The authors declare that the research was conducted in the absence of any commercial or financial relationships that could be construed as a potential conflict of interest.

Publisher's note

All claims expressed in this article are solely those of the authors and do not necessarily represent those of their affiliated organizations, or those of the publisher, the editors and the reviewers. Any product that may be evaluated in this article, or claim that may be made by its manufacturer, is not guaranteed or endorsed by the publisher.

References

Basaran, R., Efendioglu, M., Kaksi, M., Celik, T., Mutlu, I., and Ucar, M. (2019). Finite element analysis of short- versus long-segment posterior fixation for thoracolumbar burst fracture. *World Neurosurg.* 128, e1109–e1117. doi:10.1016/j.wneu.2019.05.077

Cahueque, M., Cobar, A., Zuniga, C., and Caldera, G. (2016). Management of burst fractures in the thoracolumbar spine. *J. Orthop.* 13 (4), 278–281. doi:10.1016/j.jor.2016.06.007

Cai, P., Lu, S., Yu, J., Xiao, L., Wang, J., Liang, H., et al. (2023). Injectable nanofiber-reinforced bone cement with controlled biodegradability for minimally-invasive bone regeneration. *Bioact. Mater* 21, 267–283. doi:10.1016/j.bioactmat.2022.08.009

Charles, Y. P., and Steib, J. P. (2015). Management of thoracolumbar spine fractures with neurologic disorder. *Orthop. Traumatol. Surg. Res.* 101 (1), S31–S40. doi:10.1016/j.otsr.2014.06.024

Chevalier, Y., Matsuura, M., Kruger, S., Traxler, H., Fleege, C., Rauschmann, M., et al. (2021). The effect of cement augmentation on pedicle screw fixation under various load cases: results from a combined experimental, micro-CT, and micro-finite element analysis. *Bone Jt. Res.* 10 (12), 797–806. doi:10.1302/2046-3758.1012.BJR-2020-0533.R1

Cook, E., Scantlebury, A., Booth, A., Turner, E., Ranganathan, A., Khan, A., et al. (2021). Surgery versus conservative management of stable thoracolumbar fracture: the PRESTO feasibility RCT. *Health Technol. Assess.* 25 (62), 1–126. doi:10.3310/hta25620

Elmasry, S. S., Asfour, S. S., and Travascio, F. (2018). Finite element study to evaluate the biomechanical performance of the spine after augmenting percutaneous pedicle screw fixation with kyphoplasty in the treatment of burst fractures. *J. Biomech. Eng.* 140 (6). doi:10.1115/1.4039174

Guo, H. Z., Zhang, S. C., Guo, D. Q., Ma, Y. H., Yuan, K., Li, Y. X., et al. (2020). Influence of cement-augmented pedicle screws with different volumes of polymethylmethacrylate in osteoporotic lumbar vertebrae over the adjacent segments: a 3D finite element analysis. *BMC Musculoskelet. Disord.* 21 (1), 460. doi:10.1186/s12891-020-03498-6

Hughes, H., Carthy, A. M., Sheridan, G. A., Donnell, J. M., Doyle, F., and Butler, J. (2021). Thoracolumbar burst fractures: a systematic review and meta-analysis comparing posterior-only instrumentation versus combined anterior-posterior instrumentation. *Spine (Phila Pa 1976)* 46 (15), E840–E849. doi:10.1097/BRS.0000000000003934

Kang, S., Park, C. H., Jung, H., Lee, S., Min, Y. S., Kim, C. H., et al. (2022). Analysis of the physiological load on lumbar vertebrae in patients with osteoporosis: a finite-element study. *Sci. Rep.* 12 (1), 11001. doi:10.1038/s41598-022-15241-3

Liao, J. C. (2020). Impact of osteoporosis on different type of short-segment posterior instrumentation for thoracolumbar burst fracture-A finite element analysis. *World Neurosurg.* 139, e643–e651. doi:10.1016/j.wneu.2020.04.056

Mai, H. T., Mitchell, S. M., Hashmi, S. Z., Jenkins, T. J., Patel, A. A., and Hsu, W. K. (2016). Differences in bone mineral density of fixation points between lumbar cortical and traditional pedicle screws. *Spine J.* 16 (7), 835–841. doi:10.1016/j.spinee.2015.11.034

Massey, P. A., Hoge, S., Nelson, B. G., Ogden, A. L., Mody, M. G., Myers, M., et al. (2021). Nitinol memory rods versus titanium rods: a biomechanical comparison of posterior spinal instrumentation in a synthetic corpectomy model. *Glob. Spine J.* 11 (3), 277–282. doi:10.1177/2192568220902401

Matsukawa, K., Yato, Y., Imabayashi, H., Hosogane, N., Asazuma, T., and Nemoto, K. (2015). Biomechanical evaluation of cross trajectory technique for pedicle screw insertion: combined use of traditional trajectory and cortical bone trajectory. *Orthop. Surg.* 7 (4), 317–323. doi:10.1111/os.12212

Muratore, M., Allasia, S., Viglierchio, P., Abbate, M., Aleotti, S., Masse, A., et al. (2021). Surgical treatment of traumatic thoracolumbar fractures: a retrospective review of 101 cases. *Musculoskelet. Surg.* 105 (1), 49–59. doi:10.1007/s12306-020-00644-0

Patel, S., Solitro, G. F., Sukotjo, C., Takoudis, C., Mathew, T., Amirouche, F., et al. (2015). Nanotopography and surface stress analysis of Ti6Al4V bioimplant: an alternative design for stability. *Jom* 67 (11), 2518–2533. doi:10.1007/s11837-015-1341-8

Pflugmacher, R., Schleicher, P., Schaefer, J., Scholz, M., Ludwig, K., Khodadadyan-Klostermann, C., et al. (2004). Biomechanical comparison of expandable cages for vertebral body replacement in the thoracolumbar spine. *Spine (Phila Pa 1976)* 29 (13), 1413–1419. doi:10.1097/01.brs.0000129895.90939.1e

Sakaura, H., Miwa, T., Yamashita, T., Kuroda, Y., and Ohwada, T. (2016). Posterior lumbar interbody fusion with cortical bone trajectory screw fixation versus posterior lumbar interbody fusion using traditional pedicle screw fixation for degenerative lumbar spondylolisthesis: a comparative study. *J. Neurosurg. Spine* 25 (5), 591–595. doi:10.3171/2016.3.SPINE151525

Santoni, B. G., Hynes, R. A., McGilvray, K. C., Rodriguez-Canessa, G., Lyons, A. S., Henson, M. A., et al. (2009). Cortical bone trajectory for lumbar pedicle screws. *Spine J.* 9 (5), 366–373. doi:10.1016/j.spinee.2008.07.008

Sellin, J. N., Raskin, J. S., Staggers, K. A., Brayton, A., Briceno, V., Moreno, A. J., et al. (2018). Feasibility and safety of using thoracic and lumbar cortical bone trajectory pedicle screws in spinal constructs in children: technical note. *J. Neurosurg. Pediatr.* 21 (2), 190–196. doi:10.3171/2017.7.PEDS17240

Solitro, G. F., Whitlock, K., Amirouche, F., Mehta, A. I., and McDonnell, A. (2019). Currently adopted criteria for pedicle screw diameter selection. *Int. J. Spine Surg.* 13 (2), 132–145. doi:10.14444/6018

Spiegl, U. J., Jarvers, J. S., Osterhoff, G., Kobbe, P., Holbing, P. L., Schnake, K. J., et al. (2022). Effect of subsequent vertebral body fractures on the outcome after posterior stabilization of unstable geriatric fractures of the thoracolumbar spine. *BMC Musculoskelet. Disord.* 23 (1), 1064. doi:10.1186/s12891-022-06031-z

Szczodry, M., Solitro, G. F., Amirouche, F., and Patel, P. (2018). Pedicle screw with increased cortical purchase can Be inserted with same accuracy as the screw in straightforward trajectory using 3D modeling landmarks. *Spine Deform.* 6 (1), 20–27. doi:10.1016/j.jspd.2017.06.004

Ueno, M., Imura, T., Inoue, G., and Takaso, M. (2013). Posterior corrective fusion using a double-trajectory technique (cortical bone trajectory combined with traditional trajectory) for degenerative lumbar scoliosis with osteoporosis: technical note. *J. Neurosurg. Spine* 19 (5), 600–607. doi:10.3171/2013.7.SPINE13191

Volz, M., Elmasry, S., Jackson, A. R., and Travascio, F. (2021). Computational modeling intervertebral disc pathophysiology: a review. *Front. Physiol.* 12, 750668. doi:10.3389/fphys.2021.750668

Wang, W., Baran, G. R., Garg, H., Betz, R. R., Moumene, M., and Cahill, P. J. (2014). The benefits of cement augmentation of pedicle screw fixation are increased in osteoporotic bone: a finite element analysis. *Spine Deform.* 2 (4), 248–259. doi:10.1016/j.jspd.2014.03.002

Wang, W., Pei, B., Pei, Y., Shi, Z., Kong, C., Wu, X., et al. (2019). Biomechanical effects of posterior pedicle fixation techniques on the adjacent segment for the treatment of thoracolumbar burst fractures: a biomechanical analysis. *Comput. Methods Biomech. Biomed. Engin* 22 (13), 1083–1092. doi:10.1080/10255842.2019.1631286

Wu, Y., Chen, C. H., Tsuang, F. Y., Lin, Y. C., Chiang, C. J., and Kuo, Y. J. (2019). The stability of long-segment and short-segment fixation for treating severe burst fractures at the thoracolumbar junction in osteoporotic bone: a finite element analysis. *PLoS One* 14 (2), e0211676. doi:10.1371/journal.pone.0211676

Wycisk, E., Solbach, A., Siddique, S., Herzog, D., Walther, F., and Emmelmann, C. (2014). Effects of defects in laser additive manufactured Ti-6Al-4V on fatigue properties. *8th Int. Conf. Laser Assisted Net Shape Eng. (Lane 2014)* 56, 371–378. doi:10.1016/j.phpro.2014.08.120

Zhao, Y., Liang, J., Luo, H., Xu, Y., and Lu, S. (2021). Double-trajectory lumbar screw placement guided by a set of 3D-printed surgical guide templates: a cadaver study. *BMC Musculoskelet. Disord.* 22 (1), 296. doi:10.1186/s12891-021-04149-0